Signal propagation in collisional plasma with negative ions

I. Kaganovich[a)]
Plasma Physics Laboratory, Princeton University, New Jersey 08543

S. V. Berezhnoi[b)] and C. B. Shin[c)]
Ajou University, Suwon 442-749, South Korea

(Received 21 September 2000; accepted 29 November 2000)

The transport of charged species in collisional currentless plasmas is traditionally thought of as a diffusion-like process. In this paper, it is demonstrated that, in contrast to two-component plasma, containing electrons and positive ions, the transport of additional ions in multispecies plasmas is not governed by diffusion, rather described by nonlinear convection. As a particular example, plasmas with the presence of negative ions have been studied. The velocity of a small perturbation of negative ions was found analytically and validated by numerical simulation. As a result of nonlinear convection, initially smooth ion density profiles break and form strongly inhomogeneous shock-like fronts. These fronts are different from collisionless shocks and shocks in fully ionized plasma. The structure of the fronts has been found analytically and numerically. [DOI: 10.1063/1.1346632]

I. INTRODUCTION

Discharges in electronegative gases (the sixth and seventh groups of the periodic table) form a large number of negative ions. One of the most important examples of electronegative plasmas is atmospheric electricity. Another example is discharges in halogen gases, typically used in material processing for semiconductor manufacturing.[1] In some applications, negative ion beams are preferable to positive ion beams, and discharges in electronegative gases are used as a source of negative ions.[2] The ionospheric D layer[3] is also one of the examples of atmospheric plasmas with a large percentage of negative ions. Recently, great interest has been devoted to dusty plasmas, where dust particles are negatively charged and can be viewed as large negative ions.[4]

We focus on general properties of partially ionized nonstationary collisional plasma transport where the ion mean free path is smaller than the plasma chamber dimensions. Generally, transport of charged species in multicomponent plasmas is thought to be some sort of ambipolar diffusion.[5] In this paper, it is demonstrated that, in contrast to a two-component plasma, containing electrons and positive ions, the transport of additional ions in multispecies plasmas is not governed by diffusion, rather described by nonlinear convection. Ion density discontinuities may form as a result of nonlinear convection and ion density profile break. In this paper we generalize results received in Refs. 6 and 7 for a case of current carrying plasmas. Though the front formation for currentless plasma was already proposed in Ref. 8, this paper lacked rigorous analysis of small signal propagation and good numerical examples, thus, the results were not disseminated in the plasma physics community.

The paper is organized as follows: Section II describes the main set of equations; Sec. III considers results of a linear theory of dynamics of small perturbations of negative ions in inhomogeneous partially ionized plasma; Sec. IV generalizes the results of linear theory on the nonlinear case and describes the formation of negative ion density discontinuities–fronts; Sec. V is devoted to the front structure; and Sec. VI contains the conclusion and outlook.

II. DESCRIPTION OF THE MODEL

A. System of equations

We assume that the ion mean free path is small compared to the characteristic discharge dimension and examine one-dimensional species transport in a parallel plate geometry. The charged species fluxes in collisional partially ionized plasma are described by a drift-diffusion approximation

$$\Gamma_k = -D_k \frac{\partial n_k}{\partial x} - \mu_k n_k e E,$$

where D_k and μ_k are the k-species diffusion coefficient and mobility, respectively, linked by the Einstein relation $D_k = T_k \mu_k / e$. T_k is the k-species temperature. We shall address only currentless plasma with zero net current $j = e(\Gamma_p - \Gamma_n - \Gamma_e) = 0$. Taking into consideration only one positive and one negative ion species with densities (n_p, n_n, respectively), the self-consistent electrostatic field (E) is given[5] by

$$E = \frac{D_p \nabla n_p - D_n \nabla n_n - D_e \nabla n_e}{\mu_p n_p + \mu_n n + \mu_e n_e}. \tag{1a}$$

Subscripts p, n, and e correspond to positive ions, negative ions, and electrons, respectively, and $\nabla = \partial / \partial x$. Below we shall consider only the case when the electron density is such

a)Electronic mail: ikaganov@pppl.gov
b)On leave from Physical Technical Department, St. Petersburg State Technical University, 195251, Russia. Electronic mail: berezhnoj@phtf.stu.neva.ru
c)Electronic mail: cbshin@madang.ajou.ac.kr

that $\mu_e n_e \gg \mu_n n_n, \mu_p n_p$ and its gradient is not too small ($D_e \nabla n_e \gg D_n \nabla n_n, D_p \nabla n_p$); and electrons are described by the Boltzmann equilibrium:

$$E = -T_e / e \nabla(\ln n_e), \tag{1b}$$

which gives an explicit relation between the electric field and the logarithmic electron density gradient. Even though the electron drift flux is larger than the ion drift fluxes, the electronegativity n/n_e can be large, since the ratio of mobilities is huge, of the order of a few hundreds. Equation (1b) for the electric field, along with the continuity equations for negative ion [Eq. (2a)] and positive ion number density [Eq. (2b)], and the electroneutrality constraint [Debye radius is assumed small, Eq. (3)], yield a complete system of equations that describes the spatiotemporal evolution of charged species densities, fluxes, and electric fields:

$$\frac{\partial n_n}{\partial t} - \mu_n \frac{\partial}{\partial x}\left(T_i \frac{\partial n_n}{\partial x} + eEn_n \right) = \nu_{\mathrm{att}} n_e - \nu_d n_n - \beta_{ii} n_n n_p , \tag{2a}$$

$$\frac{\partial n_p}{\partial t} - \mu_p \frac{\partial}{\partial x}\left(T_i \frac{\partial n_p}{\partial x} - eEn_p \right) = \nu_{\mathrm{ioniz}} n_e - \beta_{ii} n_n n_p , \tag{2b}$$

$$n_e = n_p - n_n . \tag{3}$$

In the above equations, β_{ii} is the ion–ion recombination rate coefficient, ν_{ioniz}, ν_{att}, and ν_d are the ionization, attachment, and detachment frequencies, respectively.

Being focused on general properties of nonlinear transport, we neglected source terms and assumed ion mobilities as constant.

The system (1)–(3) for positive and negative ion densities can be rewritten in terms of negative ion density and electron density:

$$\frac{\partial n_n}{\partial t} - \frac{\partial}{\partial x}\left(\mu_n T_i \frac{\partial n_n}{\partial x} - u_n n_n \right) = 0, \tag{4a}$$

$$\frac{\partial n_e}{\partial t} - \frac{\partial}{\partial x}\left(D_{\mathrm{eff}} \frac{\partial n_e}{\partial x} \right) - \frac{\partial}{\partial x}\left((\mu_p - \mu_n) T_i \frac{\partial n_n}{\partial x} \right) = 0, \tag{4b}$$

$$u_n \equiv \frac{\mu_n T_e}{n_e} \frac{\partial n_e}{\partial x}, \tag{5a}$$

$$D_{\mathrm{eff}}\left(\frac{n_n}{n_e} \right) = \frac{T_e(\mu_p n_p + \mu_n n_n)}{n_e} + \mu_p T_i, \tag{5b}$$

where u_n is the negative ion drift velocity, D_{eff} is the effective electron diffusion coefficient. The new system of Eq. (4) and (5) is more transparent than the initial system (2), since (4b) has only the diffusive term, in contrast to the diffusion and drift terms of Eqs. (2a) and (2b).

B. Numerical method

The system of Eqs. (1b), (2), and (3) has been solved with the finite difference method. The flux-corrected transport technique (FCT) was employed for Eq. (2). The second-order FCT method[6] was necessary to use for suppressing numerical diffusion, arising from the convection term.

In the FCT technique the first step is to calculate the initial guess (predictor) at next $(n+1)$ step in time (τ) at the jth point in space, chosen on uniform mesh with grid space (h):

$$n_j^* = n_j^n - \frac{\tau}{2h}(-u_r n_r + u_l n_l) + \nu(n_{j+1}^n + n_j^n + n_{j-1}^n),$$

where $u_r = (u_j^n + u_{j+1}^n)/2$, $u_l = (u_j^n + u_{j-1}^n)/2$, $n_r = (n_j^n + n_{j+1}^n)/2$, $n_l = (n_j^n + n_{j-1}^n)/2$, and $n_j^n \equiv n_n(n\tau, x_j)$, $u_j \equiv u_n(x_j)$, ν is numerical positive diffusion coefficient. The second step is to calculate corrector fluxes

$$f_{j+1/2}^c = \mathrm{sign}(\Delta n_{j+1/2}) \max\{0, \min[\Delta n_{j-1/2}\, \mathrm{sign}(\Delta n_{j+1/2}),$$
$$\mu|\Delta n_{j+1/2}|, \Delta n_{j+3/2}\, \mathrm{sign}(\Delta n_{j+1/2})]\},$$

where $\Delta n_{j+1/2} = n_{j+1}^* - n_j^*$, and coefficient μ determines antidiffusion. The third step calculates the value of n_j^{n+1} $n_j^{n+1} = n_j^* - f_{j+1/2}^c + f_{j-1/2}^c$.

Reference 9 recommends the following values for the single convection equation $\nu = 1/6 + C^2/3$, $\mu = 1/6 - C^2/6$, where $C = u\tau/h$. However, we found that the optimal choice of the values of μ, ν for the system of Eqs. (1b), (2), and (3) was 0.005, for the best illumination of numerical diffusion and dispersion.

III. SMALL PERTURBATION DYNAMIC

We first study the small signal propagation in unbounded uniform plasma. In gas discharges, ion temperature is a factor of 100 or less compared to electron temperature; as a result, ion diffusion may be neglected compared with drift.

The ion and electron density variations δn_α are taken to be of the form $\delta n_\alpha \exp(-i\omega t + ikx)$. Substitution of charged species variations into (4) results in

$$-i\omega\,\delta n - \mu_n T_e k^2 \frac{n}{n_e}\,\delta n_e = 0, \tag{6a}$$

$$-i\omega\,\delta n_e + D_{\mathrm{eff}} k^2\,\delta n_e = 0, \tag{6b}$$

$$\delta n_e = \delta n_p - \delta n_n . \tag{6c}$$

There are two modes. The first mode, in which the electron density remains uniform ($\delta n_e = 0$) $\delta n_p = \delta n_n$, does not evolve in time (its slow dissipation is described by the ion diffusion omitted here), and its frequency equals zero:

$$\omega_1 = 0. \tag{7a}$$

The second mode evolves with frequency

$$\omega_2 = -iD_{\mathrm{eff}} k^2. \tag{7b}$$

This mode corresponds to monotonic decay of a density perturbation with effective diffusion coefficient D_{eff}. Short wavelength modes (large k) decay more rapidly.

The evolution scenario in this case is close to the situation in the pure two component plasma with diffusion coefficient D_{eff}, instead of the ordinary ambipolar coefficient in two-component plasma $D_a \equiv \mu_p T_e$. In the limit of the two-component plasma, negative ion density equals zero and the effective diffusion coefficient (5b) coincides with the ambipolar diffusion coefficient. At large electronegativity

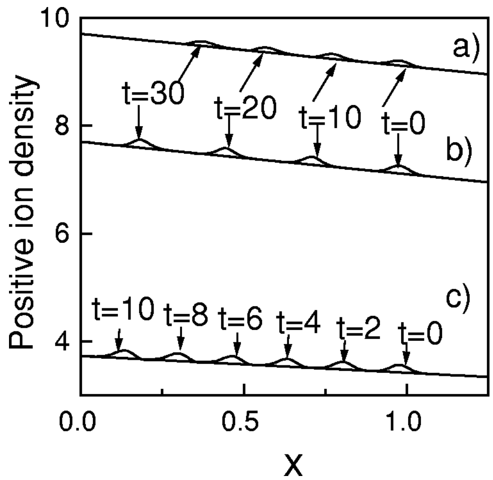

FIG. 1. Propagation of small signal for the same unperturbed electron density ($n_e=3.7-0.3x$) and different densities of unperturbed plasma negative ions. (a) $n\approx 2.0n_e$ ($n=6-0.3x$), (b) $n\approx n_e$ ($n=4-0.3x$), (c) $n=0$. All variables are dimensionless, normalized on some reference values, density n/n_0, coordinate x/L, time $tL^2/(\mu_n T_e)$. Ion diffusion was neglected, and ion mobilities were taken to be the same $\mu_n=\mu_p$.

($n_n/n_e \gg 1$), the effective diffusion coefficient (5b) is much greater than the ambipolar diffusion—the presence of the negative ions can strongly enhance the value of $D_{\rm eff}$. This property strongly influences the evolution of the electronegative plasma profiles, as will be discussed below.

The signal propagation is different, if the inhomogeneity of the background plasma is taken into account, in particular the electron density gradient: $\partial n_e/n_e\partial x \equiv 1/L_e \neq 0$. The derivations are easier to perform in the limit of small scale perturbations $|kL_e| \gg 1$. Linearization of system (4) results in a quadratic equation for frequency:

$$\omega^2+b\omega-c=0, \tag{8a}$$

$$b=-iD_{\rm eff}k^2, \quad c=-\mu_p\mu_n T_e^2 ik^3\left(\frac{\partial n_e}{n_e\partial x}\right), \tag{8b}$$

small terms of the order of $(1/kL_e)$ were neglected in (8). From the quadratic equation (8a) for frequency it follows that its roots should satisfy $(\omega_1+\omega_2)=-b$, $\omega_1\omega_2=c$. As we shall see $\omega_1 \ll \omega_2$; and then immediately $\omega_2 \cong -b$ and $\omega_1 \cong -c/b$, in the leading terms of kL_e:

$$\omega_1=u_{\rm eff}k, \quad u_{\rm eff}=\frac{\mu_n\mu_p}{\mu_n n_n+\mu_p n_p}\frac{T_e\partial n_e}{\partial x}. \tag{9a}$$

$$\omega_2=-iD_{\rm eff}k^2. \tag{9b}$$

The fast diffusive mode (7b) and (9b) $\omega=\omega_2$, remains unchanged. On the other hand, the static mode (7a) $\omega=\omega_1$ converts into a propagating one (9a). In this mode, the signal moves with the velocity $u_{\rm eff}=u_n\mu_p n_e/(\mu_n n_n+\mu_p n_p)$ factor $\mu_p n_e/(\mu_n n_n+\mu_p n_p)$ different from the negative ion drift velocity u_n.

The theoretical predictions were verified by numerical modeling. The propagation of the small perturbation is shown in Fig. 1 for three different values of electronegativities (n/n_e). When electronegativity is small ($n/n_e \ll 1$), $u_{\rm eff}$ coincides with the drift velocity of negative ions $u_{\rm eff} \approx u_n$. In the opposite case, when electronegativity is large ($n/n_e \gg 1$), $u_{\rm eff}$ is much lower than the drift velocity u, as can be seen in Fig. 1. Theoretical calculations for signal speed exactly coincide with results of numerical simulations as demonstrated in Table I.

TABLE I. (a), (b), and (c) Speed of the signal propagation ($10^{-2}u_{\rm eff}$) for the conditions of Figs. 1(a)–1(c), num. denotes the results of numerical simulations, theory–calculations by Eq. (9a).

	(a)		(b)	
Time	$u_{\rm eff}$, num.	$u_{\rm eff}$, theory	$u_{\rm eff}$, num.	$u_{\rm eff}$, theory
0	1.999	1.991	2.701	2.713
10	1.975	1.978	2.642	2.631
20	1.953	1.950	2.587	2.581
30	1.931	1.933	2.536	2.533

	(c)	
Time	$u_{\rm eff}$, num.	$u_{\rm eff}$, theory
0	8.058	8.012
2	7.933	7.964
4	7.814	7.801
6	7.703	7.701
8	7.596	7.586
10	7.496	7.501

IV. NONLINEAR EVOLUTION OF NEGATIVE ION DENSITY PROFILES AND FORMATION OF NEGATIVE ION FRONTS

As discussed above, the speed of the negative ion density perturbation depends significantly on negative ion density. As a result, different parts of the profile of large perturbations of negative ion density move with different velocity, and nonlinear evolution results in the profile modification. For analysis of the nonlinear evolution of the negative ion density profile, it is convenient to rederive the small signal propagation velocity (9a) in another way. In narrow perturbations of negative ion density (in the limit $|kL_e| \gg 1$), the electron density perturbations evolve much faster ($\omega_2 \gg \omega_1$), and electron density adiabatically adjusts itself to ion density. Consequently, electron flux varies much more slowly than ion flux, and can be assumed to be nearly constant. Using electron flux as slowly varying variable, it is convenient to substitute the electron gradient $\partial n_e/\partial x$ by electron flux $\Gamma_e=-D_{\rm eff}\partial n_e/\partial x$, Eq. (4a) can be rewritten in the form

$$\frac{\partial n}{\partial t}+\frac{\partial}{\partial x}(\Gamma_n)=0, \tag{10a}$$

$$\Gamma_n=-\Gamma_e\frac{\mu_n n}{\mu_n n_n+\mu_p n_p}, \tag{10b}$$

where the small diffusion term was neglected. Making use of slow variation of electron flux, Eq. (10a) reads

$$\frac{\partial n_n}{\partial t}+u_{\rm eff}(n_n)\frac{\partial}{\partial x}n_n=0, \quad u_{\rm eff}=\frac{\partial\Gamma_n}{\partial n_n}, \tag{10c}$$

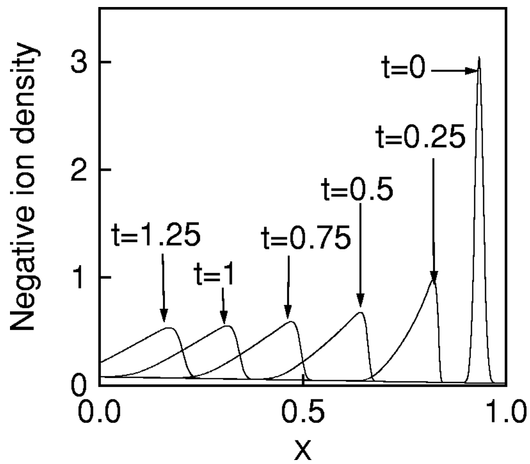

FIG. 2. Propagation of large perturbation of negative ion density for the conditions of Fig. 1, but $T_i=0.001$ and $n_e=6.2-3.6x$, initially at $t=0$ $n=(N/a\sqrt{\pi})\exp(-(x-0.93)^2/a^2)$, where $a=0.0144$, and total number of negative ions $N=0.476$, and negative ion density profiles are plotted 6 times every 0.25 units of dimensionless time.

where the small signal propagation velocity u_{eff} coincides with the previous estimate (9a), but still remains valid for nonlinear perturbations, too. The evolution of nonlinear negative ion density perturbation is shown in Fig. 2. The general theory of nonlinear convection shows,[10] that each point of initial profile $n_0(x)$ moves with its own velocity $u_{\mathrm{eff}}(n)$, and the solution of (10c) is $n=n_0(x-u_{\mathrm{eff}}(n_0)t)$.

According to the theoretical predictions, in Fig. 2 the regions of small negative ion density move faster than regions of large negative ion density. As a result the front of the profile spreads out, and steepening of the back profile leads to profile break and formation of ion density discontinuity—*ion density fronts* (Fig. 2). Note that negative ion density fronts are different from gas dynamic shocks, although both originated from nonlinear convection.

V. STRUCTURE OF NEGATIVE ION FRONTS

The analysis of the front structure can be performed in a way similar to the studies of gas dynamic shocks as described in Ref. 10. In the frame moving with the front, electron density and flux is approximately conserved:

$$\tilde{\Gamma}_e=-T_e\frac{(\mu_p n_p+\mu_n n_n)}{n_e}\frac{dn_e}{dx}-Vn_e, \tag{11}$$

where V is shock velocity, and the tilde denotes values in the front frame. From the conservation of electron flux and density, it follows, that electron density gradients to the right (+) and to the left (−) of the shock have to satisfy

$$(\mu_p p+\mu_n n)\frac{dn_e}{dx}\bigg|^{+}=(\mu_p p+\mu_n n)\frac{dn_e}{dx}\bigg|^{-}. \tag{12}$$

Similarly negative ion flux is conserved

$$\tilde{\Gamma}_n=\Gamma_n-Vn_n \tag{13a}$$

and

TABLE II. The comparison of theoretical predictions for the front speed Eq. (15b) and numerical result, performed for the conditions of Fig. 2.

Time	V, num.	V, theory
0.00	0.40	0.40
0.25	0.69	0.68
0.50	0.68	0.67
0.75	0.63	0.62
1.00	0.58	0.58
1.25	0.54	0.54

$$V=\frac{\Gamma_n|^{+}-\Gamma_n|^{-}}{n_n^{+}-n_n^{-}}. \tag{14}$$

Substituting expression for Γ_n (10b) in Eq. (14) results in

$$V=-\frac{\mu_p\mu_n n_e\Gamma_e}{(\mu_p(n_n+n_e)+\mu_n n_n)|^{+}(\mu_p(n_n+n_e)+\mu_n n_n)|^{-}}. \tag{15a}$$

Finally, after substituting the expression for electron flux we have

$$V=\frac{\mu_p\mu_n T_e\frac{dn_e}{dx}\Big|^{+}}{(\mu_p(n_n+n_e)+\mu_n n_n)|^{-}}=\frac{\mu_p\mu_n T_e\frac{dn_e}{dx}\Big|^{-}}{(\mu_p(n+n_e)+\mu_n n)|^{+}}. \tag{15b}$$

Table II demonstrates good agreement of theoretical predictions for the front speed Eq. (15b) and numerically obtained values for the conditions of Fig. 2.

In Fig. 3 the electron and negative ion fluxes are depicted. It is seen that electron flux is nearly conserved, whereas negative ion flux changes rapidly in the front, see Fig. 3(a). Convective flux Γ_n nearly coincides with Vn, showing that the whole profile moves with the speed V, see Fig. 3(b). The difference between two fluxes $\tilde{\Gamma}_n=\Gamma_n-Vn_n$ is small, and is associated with the ion diffusion, see Fig. 3(c).

Inside the front the total flux is conserved, and ion diffusion is balanced by convective flux in the frame moving with the front. Hence, Eq. (13a) takes the form

$$\tilde{\Gamma}_n=\Gamma_n-Vn_n-\mu_n T_i\frac{\partial n_n}{\partial x}. \tag{13b}$$

Substituting the expression for convective flux Eq. (10b) and front velocity (15b) we find that at the periphery where diffusive flux tends to zero

$$\tilde{\Gamma}_n=-\frac{\mu_n(\mu_p+\mu_n)n_n^{+}n_n^{-}\Gamma_e}{(\mu_p(n_n+n_e)+\mu_n n_n)|^{-}(\mu_p(n_n+n_e)+\mu_n n_n)|^{+}}$$

and diffusion flux reads

$$-\mu_n T_i\frac{dn_n}{dx}=-V(\mu_n+\mu_p)\frac{(n_n^{+}-n_n)(n_n-n_n^{-})}{\mu_p n_p+\mu_n n_n}. \tag{16}$$

Integration of (16) yields front width

$$L_{\mathrm{front}}=\frac{\mu_n T_i}{V}F\left(\frac{n_+}{n_e},\frac{n_-}{n_e},\frac{\mu_n}{\mu_p}\right), \tag{17a}$$

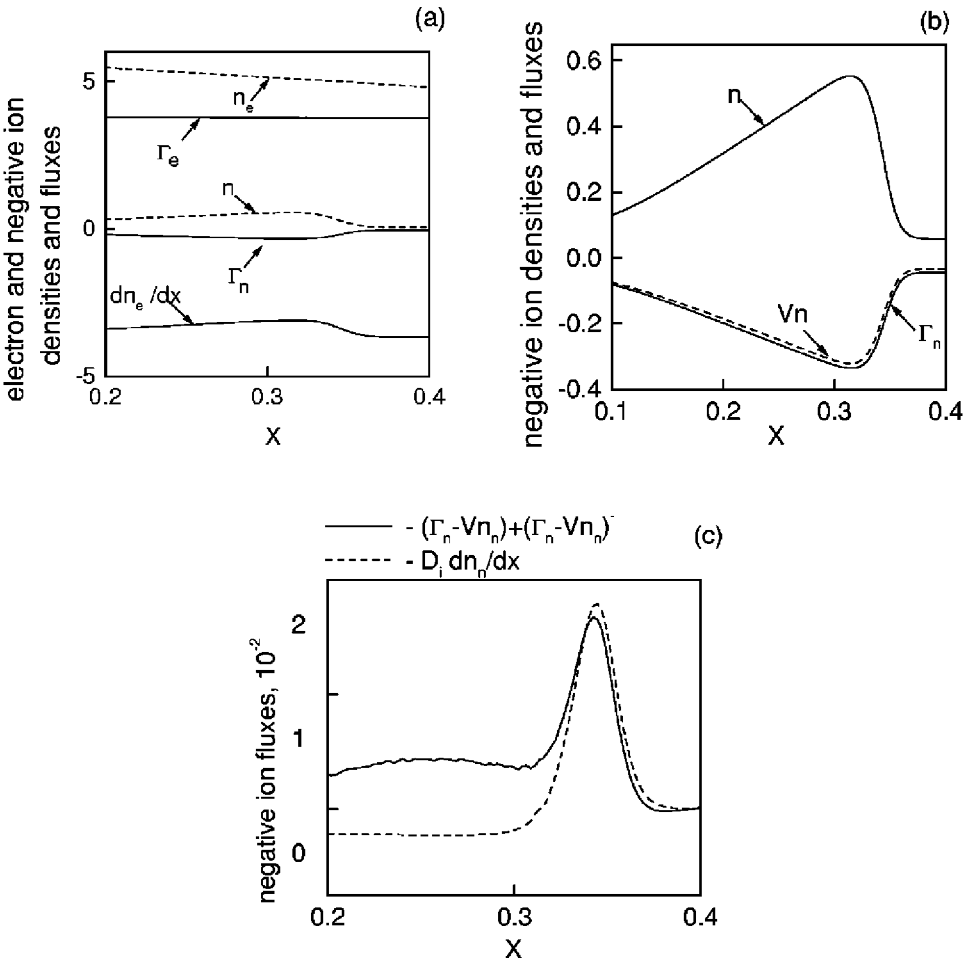

FIG. 3. Depiction of the front structure. The same conditions as in Fig. 2 at $t=1$. (a) Negative ion and electron fluxes, electron and negative ion densities and gradient of electron density, (b) convective flux Γ_n and Vn where V is front velocity from (15), (c) convective flux in the front frame $-(\Gamma_n - Vn) + (\Gamma_n - Vn)|_-$, and diffusive flux $-\mu_n T_i(\partial n/\partial x)$.

$$F\left(\frac{n_+}{n_e}, \frac{n_-}{n_e}, \frac{\mu_n}{\mu_p}\right) = \int_{s_-}^{s_+} \frac{(s+\delta)ds}{(n_+/n_e - s)(s - n_-/n_e)}, \quad (17b)$$

$$s = \frac{n - n_-}{n_e}, \quad \delta = \frac{\mu_p}{\mu_p + \mu_n} + \frac{n_-}{n_e}, \quad s_- = \varepsilon \frac{n_+ - n_-}{n_e},$$

$$s_+ = (1-\varepsilon)\frac{n_+ - n_-}{n_e},$$

where ε is an arbitrary small number. Integration of (17b) yields

$$F\left(\frac{n_n^+}{n_e}, 0, \frac{\mu_n}{\mu_p}\right) = \ln\left(\frac{1-\varepsilon}{\varepsilon}\right)\left(1 + \frac{2\delta n_e}{n_n^+}\right)$$

and front width is

$$L_{\text{front}} = \frac{\mu_n T_i}{\mu_p T_e \left.\frac{dn_e}{dx}\right|^-} \ln\left(\frac{1-\varepsilon}{\varepsilon}\right)\left(1 + \frac{2\delta n_e}{n_n^+}\right) \times (\mu_p(n + n_e) + \mu_n n)|^+ . \quad (17c)$$

In the case of equal ion mobilities, and choosing $\varepsilon = 0.1$ and $n_+ \gg n_-$

$$L_{\text{front}} = 2.2 L_e \frac{T_i}{T_e}\left(3 + \frac{n_e}{n_n^+} + \frac{n_n^+}{n_e}\right). \quad (17d)$$

For small electronegativity $n_e \gg n_+$

$$L_{\text{front}} \approx 2.2 L_e \frac{T_i}{T_e} \frac{n_e}{n_n^+},$$

front sheath is reciprocal of the change in density in the front (n_n^+); small density discontinuities spreads wider similarly to Burgers' equation[10] (where flux is the quadratic function of density).

In the opposite case of large electronegativity $n_e \ll n_+$,

$$L_{\text{front}} \approx 4.4 L_e \frac{T_i}{T_e} \frac{n_n^+}{n_e},$$

sheath width is proportional to the change in density in the front, in contrast to Burgers' equation.

In the range $1/2 < n_+/n_e < 1$ front width varies insignificantly and

$$L_{\text{front}} \approx 13 L_e \frac{T_i}{T_e}.$$

In other words, the width of the front depends upon the ratio of negative ion density and convective flux; for small electronegativity $n_e \gg n_+$ this ratio increases, and, in the opposite case of large electronegativity $n_e \ll n_+$, the ratio decreases with increase of negative ion density—front width changes, respectively.

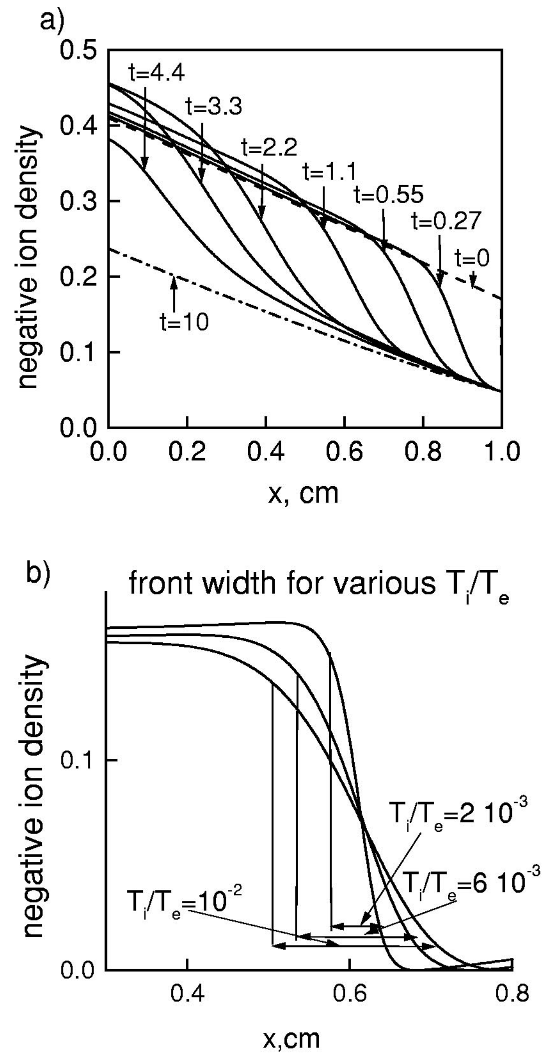

FIG. 4. Propagation of the ion density discontinuity. The initial profiles of all species are linear $n(x)=0.4-0.23x$, $n_e(x)=0.6-0.24x$, at the right boundary positive ion density was fixed $p(0)=1$, at the left boundary negative ion density was constrained initially $n(1)=0.17$; at time equal zero boundary condition on the left-hand side was changed to $n(1)=0.05$ causing ion density wave to propagate to the right-hand side. (a) depicts time evolution of perturbation for $T_i=0.001$; (b) shows perturbations of negative ion density $[n-(0.23-0.18x)]$ for three different ion temperatures, $T_i=0.002$; 0.006, 0.01. The width of the back–front of signal increases proportionally with T_i.

Comparison of theoretical estimates with numerical simulations is presented in Fig. 4 and Table III. In Fig. 4(b) one can see that the front width increases proportionally to ion temperature.

TABLE III. The comparison of theoretical predictions for the front width (17d) and numerical result, performed for the conditions of Fig. (4b). num corresponds to the width calculated as difference between positions of ion density equal to 0.9 and 0.1 of the maximum of density pertubations.

T_i/T_e	L_{front}, num.	L_{front}, theory
0.002	0.058	0.050
0.006	0.14	0.14
0.01	0.22	0.24

The examples of front formation in practical discharges are collected in a review.[11]

VI. CONCLUSIONS

In the general case of multispecies plasmas the field-driven fluxes of the charged particles are of a complex nature. Assuming a two-component plasma (positive ions and electrons with densities $n_p=n_e$), and Boltzmann equilibrium for electrons, the drift flux of positive ions is reduced to an effective linear (ambipolar) diffusion flux. If the plasma consists of two or more sorts of ions, the flux of any given species of the charged particles depends, in general, not only on its own density gradient, but also on the density gradients of all the other species. For example, the presence of negative ions substantially influences the charged species fluxes. In a plasma containing negative ions (with density n_n), the drift flux of negative ions is a nonlinear function of densities, $-\mu_n n_n E=\mu_n T_e n_n \partial \ln n_e/\partial x$, and described by convection, with a velocity that depends nonlinearly on electron densities, and via equation for evolution of electron densities depends nonlinearly on the negative ion density also. We show that in inhomogeneous EN plasmas the small-localized perturbation of positive and negative ion density moves with velocity

$$u_{\mathrm{eff}}=\frac{\mu_n\mu_p}{\mu_n n_n+\mu_p n_p}T_e\frac{\partial n_e}{\partial x}.$$

Since u_{eff} is a function of negative ion density, the nonlinear evolution of perturbations results in formations of negative ion density discontinuities—negative ion density fronts, analogous to shocks, which are widely known in gas dynamics,[10] and collisional multispecies plasmas, carrying dc current, see Refs. 6 and 7. Ion density discontinuities form as a result of nonlinear convection and ion density profile break. In this paper we have generalized the results received in Ref. 6 for a case of currentless plasmas. The width of the negative ion front is found to be proportional to the ratio of ion and electron temperatures times electron inhomogeneity scale.

In summary, plasma with negative ions tends to stratify into regions with the presence of negative ions, and in electropositive plasmas (without negative ions) the boundary between two regions, the front, is narrow and forms as a result of nonlinear convection and negative ion density profile breaking. The front is a general phenomenon for collisional multispecies plasma and has to be accounted for in the study of discharge in electronegative gases.[11]

ACKNOWLEDGMENTS

The helpful comments of Y. Raitses and E. Startsev are greatly appreciated. Authors also thank Professor R. N. Franklin, Professor A. J. Lichtenberg, and Professor L. D. Tsendin for persistent encouragement to accomplish this paper.

The work of I. Kaganovich was funded by the Princeton Plasma Physics Laboratory (University Collaboration Grant), National Science Foundation, Chemical Transport Systems CTS-9713262, and by Alexander von Humboldt Foundation. S. Berezhnoi was supported by Korea Institute of Science &

Technology Evaluation and Planning (KISTEP) program 99RE06-016, International Association of European Union, INTAS Grant No. 96-0235, and by a Russian program in thermonuclear synthesis UTS Grant No. 378. Korea Science and Engineering Foundation (KSEF) Grant No. 971-1107-018-2 supported the work of C. B. Shin.

[1] M. A. Lieberman and A. J. Lichtenberg, *Principles of Plasma Discharges and Materials Processing* (Wiley, New York, 1994).
[2] M. Hopkins and K. Mellon, Phys. Rev. Lett. **67**, 449 (1991).
[3] W. Swider, *Ionospheric Modeling* (Birkhauser Verlag, Basel, 1988), p. 320.
[4] V. N. Tsytovich, Comments Plasma Phys. Control. Fusion **1**, 41 (1999).
[5] H. Massey, *Negative Ions*, 3rd ed. (Cambridge University Press, Cambridge, 1976), p. 741.
[6] A. P. Dmitriev, V. A. Rozhansky, and L. D. Tsendin, Sov. Phys. Usp. **28**, 467 (1985).
[7] V. A. Rozhansky and L. D. Tsendin, *Transport Phenomena in Partially Ionized Plasma* (Gordon & Breach, New York, 2000), p. 320; (in Russian: Energoatomizdat, Moscow, 1988), p. 380.
[8] I. D. Kaganovich and L. D. Tsendin, Plasma Phys. Rep. **19**, 645 (1993).
[9] J. P. Boris and D. L. Brook, J. Comput. Phys. **68**, 127 (1987).
[10] G. B. Whitham, *Linear and Nonlinear Waves* (Wiley, New York, 1974), p. 220.
[11] I. D. Kaganovich, Phys. Plasmas (to be published).